Back

Water Resources Research

Regular Article | Free Access

Effect of compressibility on the rise velocity of an air bubble in porous media

Abdullah Cihan, M. Yavuz Corapcioglu

First published: 09 April 2008 | https://doi.org/10.1029/2006WR005415 | Citations: 8

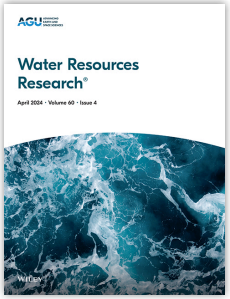

Volume 44, Issue 4
April 2008

Figures References Related Information

Recommended

Rise velocity of an air bubble in porous media: Theoretical studies

M. Yavuz Corapcioglu, Abdullah Cihan, Mirna Drazenovic

Water Resources Research

Abstract

[1] The objective of this study is to develop a theoretical model to analyze the effect of air compressibility on air bubble migration in porous media. The model is obtained by

Back

presented for various cases of interest. The model results compare favorably with both experimental data and analytical solutions reported in the literature obtained for an incompressible air bubble migration. The results show that travel velocity of a compressible air bubble in porous media strongly depends on the depth of air phase injection. A bubble released from greater depths travels with a slower velocity than a bubble with an equal volume injected at shallower depths. As an air bubble rises up, it expands with decreasing bubble pressure with depth. The volume of a bubble injected at a 1-m depth increases 10% as the bubble reaches the water table. However, bubble volume increases almost twofold when it reaches to the surface from a depth of 10 m. The vertical rise velocity of a compressible bubble approaches that of an incompressible one regardless of the injection depth and volume as it reaches the water table. The compressible bubble velocity does not exceed 18.8 cm/s regardless of the injection depth and bubble volume. The results demonstrate that the effect of air compressibility on the motion of a bubble cannot be neglected except when the air is injected at very shallow depths.

porous medium: Experimental studies

Sharon E. Roosevelt, M. Yavuz Corapcioglu

Water Resources Research

A new bubble dynamics model to study bubble growth, deformation, and coalescence

C. Huber, Y. Su, C. T. Nguyen, A. Parmigiani, H. M. Gonnermann, J. Dufek

Journal of Geophysical Research: Solid Earth

1. Introduction

[2] The vertical transport of air bubbles in granular media has important inferences in various studies such as application of in situ air sparging for groundwater remediation and ebullition of green house gases stored in deep geological formations to the atmosphere [*Pankow et al.*, 1993; *Oldenburg and Lewicki*, 2006; *Amos and Mayer*, 2006]. Transport of air in granular media can take place either in the form of discrete air channels or discrete air bubbles. In heterogeneous subsurface conditions, one flow pattern may change to the other, or a mixed (bubble channel) flow pattern may occur.

Back

[3] In situ air sparging is the direct injection of compressed air into the formation beneath the water table. As the air rises through the saturated aquifer, the volatile compounds dissolved in the water diffuse into the air and are then carried into the unsaturated zone above the water table. Here they are removed, typically by soil vapor extraction which uses vacuum extraction wells to draw the vapors out of the soil. Rise velocity of air bubbles is a critical factor in in situ air sparging operations in coarse porous media. ***Corapcioglu et al.* [2004]** used a force balance approach to model the rise velocity of a single air bubble assuming the incompressibility of the air in the bubble. The results compared favorably with experimental data reported in the literature. ***Corapcioglu et al.* [2004]** stated that air bubble expansion due to the pressure decrease in a ~1-m column was negligible, and thus bubbles traveled at their terminal velocities. ***Oldenburg and Lewicki* [2006]** employed ***Corapcioglu et al.*'s [2004]** model for incompressible bubbles to predict rise velocity of CO_2 bubbles in coarse porous media leaking due to buoyancy from deep geologic CO_2 storage sediments. However, neglecting compressibility of gas bubbles rising from deep sediments may considerably affect analyses made to understand biochemical interaction of bubbles with surrounding environment [***Amos and Mayer*, 2006**].

[4] In general, air bubbles can shrink because of mass loss by air diffusion across the bubble surface or expand because of pressure decrease as they rise in water, and thereby their velocity may change [***LeBlond*, 1969**]. Compressibility is a measure of volume changes when a substance is subjected to changes in normal pressure or tensions, and quantified by the compressibility coefficient. The compressibility coefficient under isothermal conditions is defined by $\beta = -1/\forall d\forall/dP$ where $\forall$ is the volume of a given substance and P is pressure. The minus sign indicates a decrease in volume as pressure increases. Bubble volume varies by changes in pressure due to changes in depth or

Back

bubble volume because of the solute diffusion into the bubble [*Bankoff*, 1972; *Li and Yortsos*, 1995]. In bubbly flow of air phase in saturated porous media, as air bubbles rise from an injection point, the volume of the bubbles can increase with decline in pressure toward the surface. Larger bubbles generally rise faster than smaller bubbles since the effect of buoyancy increases with the bubble volume [*Corapcioglu et al.*, 2004]. Growth of air bubbles during the air sparging operations in coarse porous media also affects the air saturation below the water table, which in turn results an increase in contaminant mass transfer across the air-water interface.

[5] The objective of this study is to model the rise of a compressible air bubble in an otherwise water-saturated porous medium. We will obtain an equation of motion for the vertical movement of individual air bubbles whose equivalent radii range between 2 and 5 mm taking into consideration the changes in bubble volume and pressure as the bubble rises. Model results for a compressible bubble will be compared with the previous results presented for an incompressible bubble by *Corapcioglu et al.* [2004].

2. Bubble Motion Equation

[6] Conservation of linear momentum equation can be stated for an air bubble rising in an otherwise saturated porous medium as

$$\frac{d}{dt}\left(\rho_g \forall_b \, \boldsymbol{u_b}\right) = \boldsymbol{F_A} + \boldsymbol{F_b} + \boldsymbol{F_d} + \boldsymbol{F_{st}} \qquad (1)$$

where $\boldsymbol{u_b}$ is the velocity of bubble, ρ_g is the density of the bubble, $\forall_b$ is the volume of the bubble, and t is the time. The right-hand side of **equation (1)** represents the sum of the

Back

to density differences between air and water phases is defined by

$$F_b = (\rho_f - \rho_g)\forall_b g \quad (2)$$

where ρ_f is the density of fluid in which bubble moves, i.e., water in this study, and g is the gravitational acceleration. ***Corapcioglu et al.*** **[2004]** used the ***Ergun*** **[1952]** equation to express the drag force including viscous and kinetic energy losses. A constant coefficient A, which was used as a correction parameter to incorporate the medium-specific properties as well as the partial contact of the bubble with solids such as the shape factor, surface area, and tortuosity to adjust the momentum transfer between the phases, was also introduced in the formulation. ***Corapcioglu et al.*** **[2004]** obtained A = 26.8 by matching the experimental data for individual bubbles whose equivalent bubble radii range between 2–5 mm in a 4 mm glass bead medium. The modified equation given by ***Corapcioglu et al.*** **[2004]** to represent the drag force will be used in this study as well.

$$F_d = F_{vd} + F_{kd} = -A\left[\frac{150\mu_b}{d_p^2}\frac{(1-\phi)^2}{\phi^3}u_b + \frac{1.75\rho_g}{d_p}\frac{(1-\phi)}{\phi^3}|u_b|\,u_b\right]\forall_b \quad (3)$$

where μ_b is the effective dynamic viscosity of the bubble, ϕ is the porosity, and d_p is the mean particle diameter.

[7] The added mass and the surface tension forces will be slightly modified in this study to incorporate the effect of air compressibility and the differences in advancing and receding contact angles. The added mass force is the additional inertial force resulting

Back

driven flow of an air bubble in an incompressible fluid [*Batchelor*, 2000], the added mass force is expressed by

$$F_A = -\rho_f \frac{d}{dt}\left(C_M \forall_b \, u_b\right) \quad (4)$$

The effect of additional added mass is a virtual increase in the particular mass by ($C_M\rho_f/\rho_g$) where C_M is the added mass coefficient that depends on the geometry of the bubble.

[8] The net surface tension force in the vertical direction due to hysteresis of contact angle is expressed by

$$F_{st} = -2\pi R'\sigma\left[\cos(\theta_R) - \cos(\theta_A)\right] \quad (5)$$

where σ is the surface tension, θ_R and θ_A are the receding and advancing contact angles of gas-liquid-solid interfaces with the vertical (Figure 1a), and R' is the equivalent radius of a pore throat through which a bubble can pass in a particular arrangement of grains (Figure 1b). Angles θ_R and θ_A can be reasonably estimated by $\theta_R = \theta - \pi/18$ and $\theta_A = \theta + \pi/18$ [*Winterton*, 1984], where θ is the equilibrium contact angle. Substituting the relationships for θ_R and θ_A, equation (5) can be rewritten as

$$F_{st} = -4\pi R'\sigma \sin(\pi/18)\sin(\theta) \quad (6)$$

Back

cubical tetrahedral model has approximately the same porosity, 0.39, as the randomly packed 4-mm glass bead medium where *Corapcioglu et al.*'s [2004] experimental data were collected.

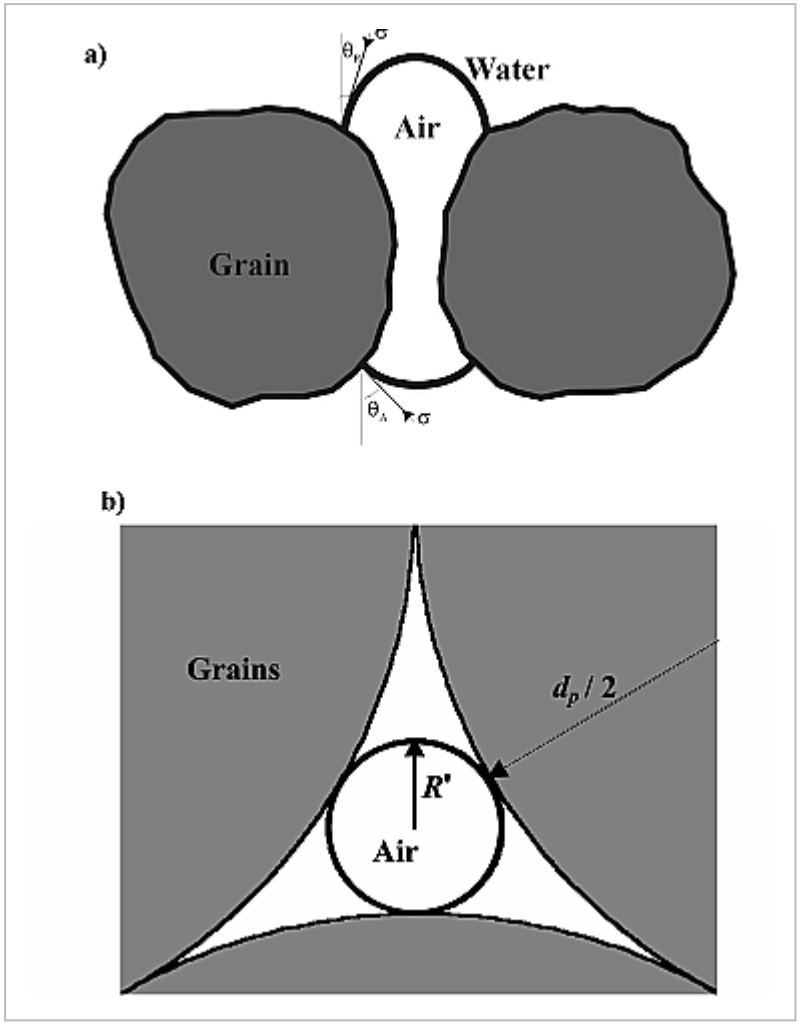

Back

bubble in a porous medium with cubical tetrahedral packing arrangement [*Corapcioglu et al.*, 2004].

[9] By substituting --(4) and (6) into equation (1) and rearranging, the governing equation for the rise velocity of a bubble $\boldsymbol{u_b}$ can be expressed in terms of vertical distance traveled by the bubble center $z(t)$ as

$$(C_M\rho_f+\rho_g)\left(\frac{d^2z}{dt^2}+\frac{1}{\forall_b}\frac{d\forall_b}{dt}\frac{dz}{dt}\right)+\frac{d\rho_g}{dt}\frac{dz}{dt}=(\rho_f-\rho_g)g$$
$$-\frac{4\pi R'\sigma\sin(\pi/18)\sin(\theta)}{\forall_b}-A\left[\frac{150\mu_b(1-\phi)^2}{d_p^2\phi^3}\frac{dz}{dt}+\frac{1.75(1-\phi)}{d_p\phi^3}\rho_g\left(\frac{dz}{dt}\right)^2\right] \quad (7)$$

where $dz/dt = u_b$ is the vertical velocity at the center of the bubble. In order to complete the derivation, we need to find relationships for bubble volume and density change in (7), which will be defined in the next section.

3. Expansion of an Air Bubble

[10] For gas bubbles moving in a liquid such as water, volume changes are caused primarily by changes in pressure due to changes in depth and/or surface tension, or by gas diffusion across the bubble surface [*Garrettson*, 1973]. For bubbles that contain n moles of ideal gas at temperature T and pressure P, the ideal gas law is expressed by

$$P\forall_b = nRT \quad (8)$$

Back

$$\rho_g = \frac{P}{R_g T} \quad (9)$$

where R_g is the gas constant for air and equal to R divided by the molecular weight of air; that is, R_g = 287.05 J kg^{-1} K^{-1}. Molecular weight of air calculated from the average composition of dry air [*Bird et al.*, 2002] is equal to 0.02897 kg/mol. The use of ideal gas law becomes unrealistic for increasing values of density especially when a bubble movement is mainly density driven where appreciable pressures can cause significant departures from the ideal gas law. The ideal gas law can be assumed applicable for −23.15°C ≤ T ≤ 726.85°C and 0.01 atm ≤ P ≤ 100 atm [*Hilsenrath et al.*, 1955].

[11] By differentiating both sides of **equation (8)** at constant temperature, we obtain

$$P\, d\forall_b + \forall_b\, dP = R\, T\, dn \quad (10)$$

The pressure in an ideal gas mixture bubble can be represented as sum of atmospheric pressure P_o, hydrostatic water pressure and capillary pressure,

$$P = P_o + \rho_f g(L - z) + \frac{4\,\sigma \sin(\pi/18)\,\sin(\theta)}{R'}; \quad 0 \le z \le L \quad (11)$$

Back

[12] By employing **equation (8)** and the definition of compressibility as given before, the compressibility coefficient β becomes equal to $1/P$ for a constant n mole (i.e., $dn = 0$) mixture of ideal gases in the bubble. This leads to a conclusion that β should increase with decreasing pressure in the bubble. In the absence of any solutes in the water phase and their vapors in the air phase, mass loss from the air phase occurs because of air diffusion into the water phase. Because of the consideration of large air bubbles released at shallow depths, the gas diffusion into the water is neglected; that is, $dn \approx 0$. However, the effect of solutes present in liquid may be significant, despite the high bubble velocities [***Levich*, 1962**]. For $dn = 0$, dividing **equation (10)** by dt and employing the chain rule of differentiation, the temporal change of the bubble volume can be expressed as

$$\frac{d\forall_b}{dt} = -\frac{\forall_b}{P}\frac{dP}{dt} = \frac{\forall_b^2 \rho_f g}{M R_g T}\frac{dz}{dt}; \qquad \forall_b(0) = \forall_{ib} \quad (12)$$

where M is the mass of the bubble. The air mass in the bubble can be calculated from the ideal gas law for a known value of the initial bubble volume $\forall_{ib}$ and pressure P_i at the injection point $z = 0$; that is, $M = P_i \forall_{ib}/(R_g T)$. Since the mass of the bubble is assumed to be constant [$d(\rho_g \forall_b)/dt \cong 0$], then **equation (7)** becomes

Back

$$+\frac{4\pi R'\sigma \sin(\pi/18)\sin(\theta)}{\forall_b} = \left(\rho_f - \frac{M}{\forall_b}\right) g \quad ; \quad 0 \le t \le t_L, 0 \le z \le L \tag{13}$$

where t_L is the time needed for a bubble reach to the water table surface. The equation (13) is bounded only from an injection point $z = 0$ to the water table surface $z = L$. When the bubble initially begins to rise from rest, initial conditions are given as

$$\left.\frac{dz}{dt}\right|_{t=0} = 0 \qquad z\Big|_{t=0} = 0 \tag{14}$$

Equations (12) and (13) form a system of nonlinear ordinary differential equations in terms of z and $\forall_b$ with initial conditions given by equations (14). An explicit solution for this initial value problem is not available except for some simplified cases which will be discussed later.

4. Numerical Solution

[13] To implement the numerical solution, equations (12) and (13) was represented as a first-order system of equations and solved by a MATLAB solver ODE 23tb which uses an implicit Runge-Kutta method. The method chosen can employ very small step sizes to achieve low error tolerances and approach the solution very fast. The parameters used in the model are given in Table 1 and are the same values used by *Corapcioglu et al.* [2004].

Back

Parameters	Units	Values
A	Dimensionless	26.8
C_M	Dimensionless	11/16
μ_b	N.s/m^2	1.8×10^{-5}
μ_f	N.s/m^2	1×10^{-3}
ρ_g	kg/m^3	1.23
ρ_f	kg/m^3	997.3
σ	N/m	7.2×10^{-2}
g	m/s^2	9.81
ϕ	%	39.54
θ	radian	$\pi/6$
d_p	m	0.004
T	K°	293.16
P_0	N/m^2	101.3×10^3

[14] The results of the numerical solution for a compressible bubble were compared with the experimental data given by ***Corapcioglu et al.* [2004]** which can be expressed in terms of depth versus time for R_i = 2 mm (**Figure 2**). The initial bubble radius, R_i is defined as the

Back

0.99, which indicates a very good match. However, as stated before since the compressibility effect is negligible for such a short column, ~0.8 m, this comparison of the numerical solution with the experimental data is given only for verification purposes and may not be useful to compare the theoretical model with experimental testing of the compressible bubble migration. Experimental testing of the compressibility effect on the rise velocity of air bubbles is not an easy task. A more meaningful comparison can be possible by conducting laboratory experiments in columns taller than 5 m in a way similar to the experiment conducted by ***Corapcioglu et al.*** **[2004]** in short columns. Such an extensive work is beyond the scope of this study.

Back

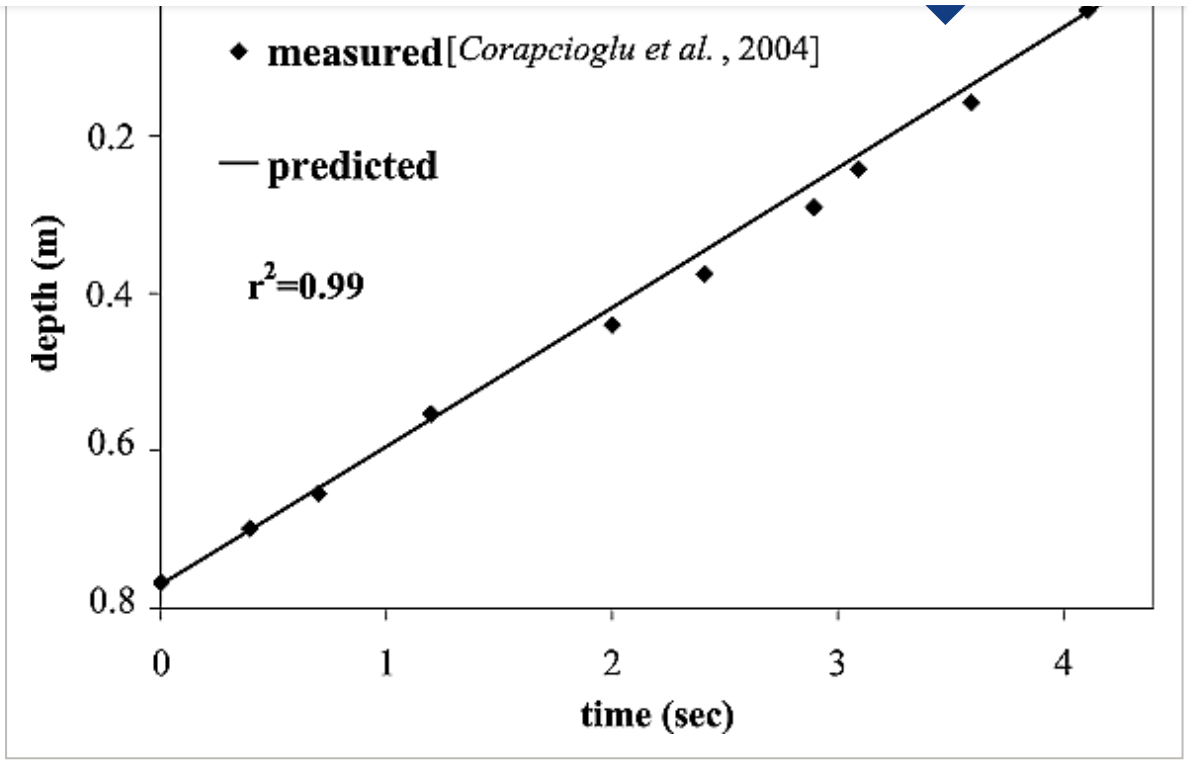

Figure 2 Open in figure viewer | PowerPoint

Comparison of numerical solution with experimental data of ***Corapcioglu et al.*** [2004] expressed in terms of distance and time for R_i = 2 mm.

[15] A general representation of the solution is shown in Figure 3 for different injection depths. The bubble injected from 10 m which is under greater initial pressure rises at a slower rate, but regardless of the injection depth all bubbles arrive at the water table surface with approximately the same velocity, i.e., ~18.8 cm/s (Figure 3a). Because of

Back

water table surface.

Back

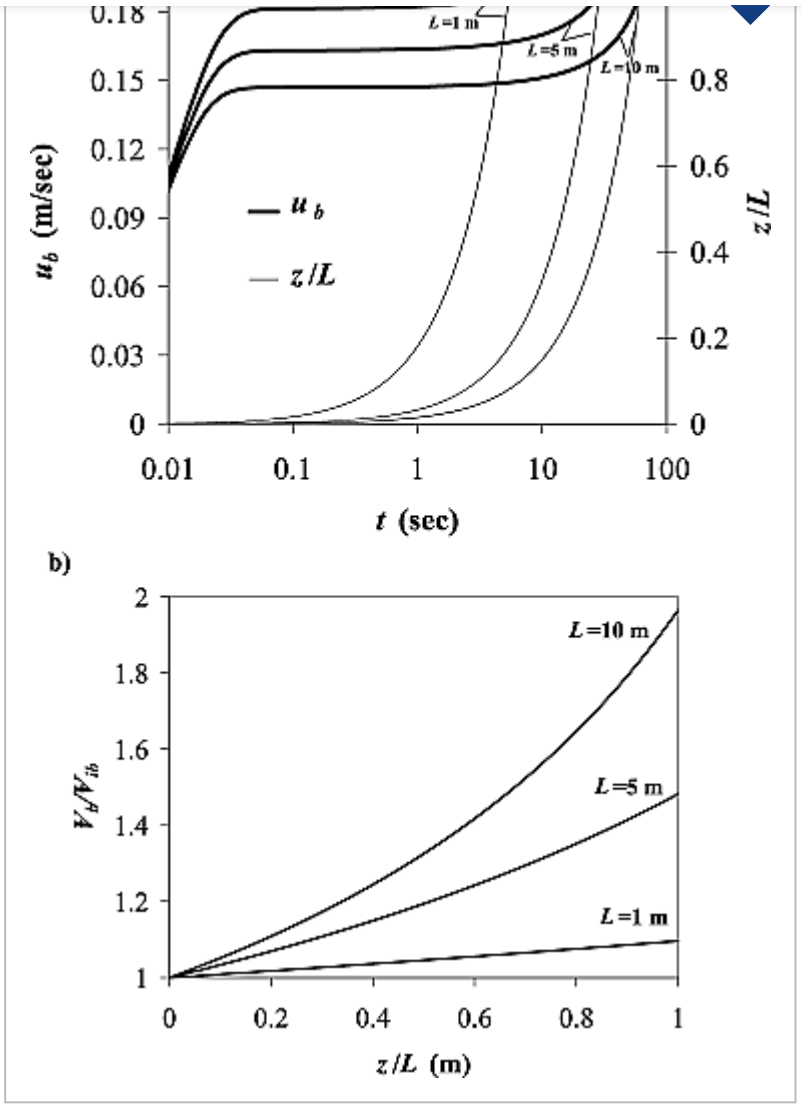

Figure 3

Open in figure viewer | PowerPoint

Back

[16] Figure 3b shows the changes in volumes of bubbles released at different depths as function of normalized depth. As the bubble rises up, it expands with decreasing pressure. Volume of a bubble injected at a 1-m depth increases 10% as the bubble reaches the water table. However, bubble volume increases almost twofold when it reaches to the surface from a depth of 10 m.

[17] Figures 4a and 4b present comparisons of compressible and incompressible bubble motions. The differences in travel distances of the bubbles at any time become larger as the injection depth L increases (Figure 4a). Compressible bubble reaches to the top surface at a later time because of its slower motion in greater depths. The incompressible bubble velocity which is independent of the injection depth shows a very similar variation with normalized depth to the compressible bubble velocity injected from 1-m depth (Figure 4b). This is not surprising since the compressibility effect is negligible at very shallow depths.

Back

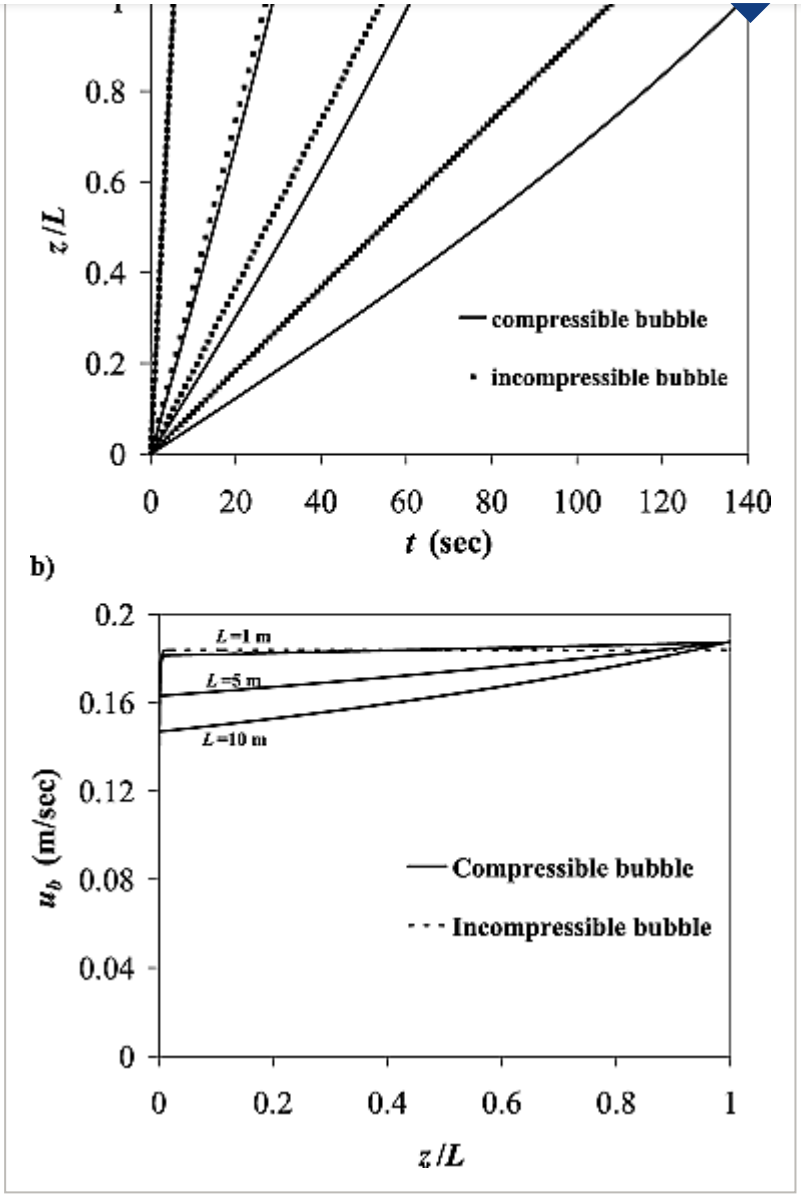
0.8
0.6
z /L
0.4
0.2
0
compressible bubble
incompressible bubble
0
20
40
60
80
100
120
140
t (sec)
b)
0.2
L=1 m
L=5 m
0.16
L=10 m
0.12
u_b (m/sec)
0.08
Compressible bubble
Incompressible bubble
0.04
0
0
0.2
0.4
0.6
0.8
1
z /L

Back

distance versus time and (b) bubble velocity as a function of dimensionless distance.

[18] The individual forces were evaluated to obtain a comparison of their respective effect on compressible bubble motion. Since the only driving force is the buoyant force, all others (F_i, F_{st}, F_{vd}, F_{kd}) were normalized by F_b. The total inertial force including the added mass force, F_i is expressed by two separate terms to individually identify second-order and first-order derivatives of z; that is,

$$F_i = F_{i1} + F_{i2} = (C_M \rho_f + \rho_g) \forall_b \frac{d^2 z}{dt^2} + \frac{C_M \rho_f^2 g \forall_b}{\rho_g R_g T} \left(\frac{dz}{dt}\right)^2 \quad (15)$$

The first term F_{i1} contains the acceleration of the bubble, and the second term F_{i2} contains the square of the velocity. Figure 5 shows variation of the normalized forces acting on a bubble with R_i = 4 mm from an injection point at 10-m depth. At very early travel distances, $z = 10^{-4}$ m, the first term of the inertial force, F_{i1} is the most dominant force that is almost 80% of the driving buoyant force. Within a short travel distance such as z = 1 m, the inertial force F_{i1} reduces sharply while the drag forces increase. Because of the expansion of the bubble and increase in rise velocity, the second term F_{i2} increases slightly, but the overall effect of both the inertial forces during the entire distance is negligible. During the rise of a compressible air bubble, the viscous drag force, F_{vd} is the most dominant one. When the bubble reaches to the surface, the kinetic drag force, F_{kd} approaches the viscous drag force, and total drag force is about 90% of the buoyant force. With the expansion of the bubble, the contribution of surface tension (less than 1%) compared to the buoyancy decreases with distance toward the water table surface (Figure 5). However, F_{st}/F_b increases for bubbles of smaller volume since the buoyancy

Back

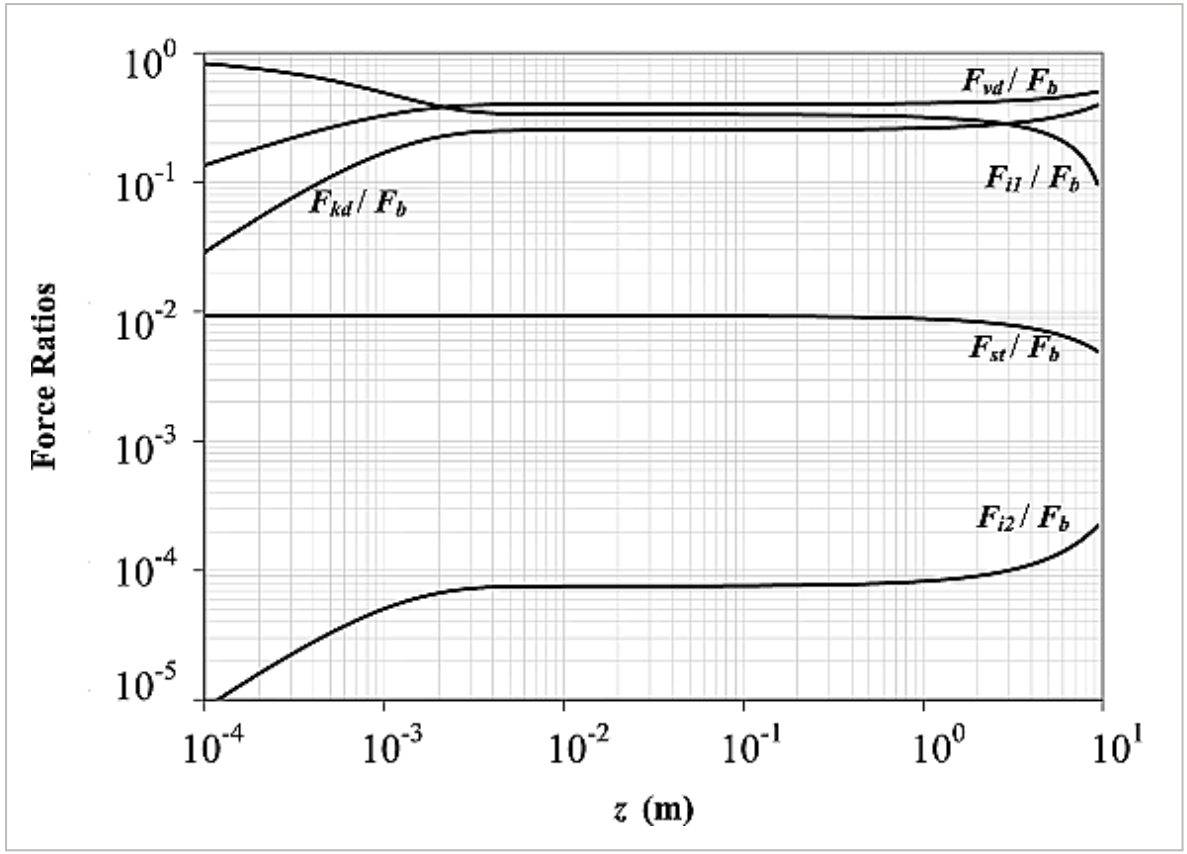

Figure 5 Open in figure viewer | PowerPoint

Effect of individual forces acting on a bubble with R_i = 4 mm released from 10 m.

[19] When a bubble is trapped among the grains of a porous medium and cannot rise, the surface tension force is equal to the driving buoyant force. Then, the limiting bubble

Back

and pressure. In other words, smaller bubbles can be released at shallower depths. However, this effect is negligible for buoyancy driven rise of bubbles from relatively shallow depths considered in this study. Numerical calculations with the parameters listed for a specific medium in Table 1 show that bubble rise does not occur for initial equivalent bubble radius $R_i < 0.84$ mm.

5. Analytical Solutions

5.1. Incompressible Bubble Motion

[20] When the compressibility of the bubble is neglected ($d\rho_g/dt \equiv 0$, $\forall_b$ = constant), the bubble velocity can be expressed as a function of time [*Corapcioglu et al.*, 2004]

$$\frac{dz}{dt} = u_b = -\frac{2C_3 \tanh\left(\frac{t}{2}\sqrt{C_2^2 - 4C_1C_3}\right)}{\sqrt{C_2^2 - 4C_1C_3} + C_2 \tanh\left(\frac{t}{2}\sqrt{C_2^2 - 4C_1C_3}\right)} \quad (16)$$

Integration of equation (16) with respect to time with the initial condition ($z = 0$ at $t = 0$) provides the vertical distance the bubble has traveled.

Back

$$2C_1\left[\left[C_2^2-2C_1C_3\cosh\left(t\sqrt{C_2^2-4C_1C_3}\right)\right]+\ln\left[\frac{\sqrt{C_2^2-4C_1C_3}-C_2\tanh\left(\frac{t}{2}\sqrt{C_2^2-4C_1C_3}\right)}{\sqrt{C_2^2-4C_1C_3}+C_2\tanh\left(\frac{t}{2}\sqrt{C_2^2-4C_1C_3}\right)}\right]\right\} \quad (17)$$

where the coefficients C_1, C_2 and C_3 are given by

$$C_1=\frac{A\ 1.75\,(1-\phi)}{d_p\phi^3\,(1+C_M\rho_f/\rho_g)},\quad C_2=\frac{A\ 150\mu_b\,(1-\phi)^2}{d_p^2\phi^3\,(\rho_g+C_M\rho_f)},$$

$$C_3=\frac{4\pi R'\sigma\sin(\pi/18)\sin(\theta)}{\forall_b\,(\rho_g+C_M\rho_f)}-\frac{(\rho_f-\rho_g)\,g}{\rho_g+C_M\rho_f} \quad (18)$$

[21] Figure 4b shows a comparison of the analytical solution for an incompressible bubble with the numerical solutions obtained for a compressible air bubble. For a 1-m column, the compressible bubble velocity is only slightly different from incompressible bubble velocity. As seen in Figures 4a and 4b, the effect of air compressibility is significant for bubbles released from greater depths. Figure 4b shows that the incompressible bubble velocity is independent of the injection depth.

5.2. Compressible Bubble Motion by Neglecting the Inertial Forces

Back

the inertial forces, the equation of motion (13) using equations (9), (11) and (12) collectively becomes

$$\frac{A\,1.75\,(1-\phi)}{d_p\,\phi^3 R_g T}(\Delta P-\rho_f g z)\left(\frac{dz}{dt}\right)^2+\frac{A\,150\mu_b(1-\phi)^2}{d_p^2\,\phi^3}\frac{dz}{dt}$$
$$-\left(\rho_f-\frac{\Delta P-\rho_f g z}{R_g T}\right)g+\frac{4\pi R'\sigma\sin(\pi/18)\sin(\theta)}{\forall_b}=0 \quad (19)$$

where $\Delta P = P_o + \rho_f g L + \frac{4\sigma \sin(\pi/18)\sin(\theta)}{R'}$. The solution for dz/dt can be written as

$$\frac{dz}{dt}=u_b=\frac{-C_6+\sqrt{C_6^2+4\,(C_4-C_5 z)(C_8+C_7 z)}}{2\,(C_4-C_5 z)},\ 0\le z\le L \quad (20)$$

where the constant coefficients C_4, C_5, C_6, C_7 and C_8 are expressed as

Back

$$C_6 = \frac{A\ 150\mu_b (1-\phi)^2}{d_p^2 \phi^3},\quad C_7 = \rho_f\, g \left[\frac{g}{R_g\, T} + \frac{4\pi\, R' \sigma\ \sin(\pi/18)\sin(\theta)}{\forall_{ib}\, \Delta P}\right],$$

$$C_8 = g\left(\rho_f - \frac{\Delta P}{R_g\, T}\right) - \frac{4\pi\, R' \sigma\ \sin(\pi/18)\sin(\theta)}{\forall_{ib}} \qquad (21)$$

[23] A plot of equation (20) for a bubble injected from a 10-m depth is given in Figure 6 along with a comparison with the numerical solution incorporating the inertial forces for bubbles with R_i = 4 mm. Figure 6 shows that the analytical solution given by equation (20) slightly differs from the numerical solution, and suggests that the rise velocity of compressible bubbles can be predicted by employing equation (20). The distance z traveled by the bubble at any time t can be obtained by numerically integrating equation (20). Equation (20) can be further simplified by expanding in a Taylor series around z = 0 up to the second-order terms

$$u_b = \frac{-C_6 + \sqrt{C_6^2 + 4\,C_4\,C_8}}{2\,C_4} + \frac{z}{2\,C_4^2}\left[-C_5\,C_6 + \frac{2\,C_4^2 C_7 + C_5\,(C_6^2 + 2\,C_4 C_8)}{\sqrt{C_6^2 + 4\,C_4 C_8}}\right] + O\left(z^2\right) \qquad (22)$$

Back

shallower depths, less than 5 m. The travel time can be calculated as function of z by integrating **equation (22)** from $z = 0$ to z

$$t = \frac{2C_4^2\sqrt{C_6^2 + 4C_4C_8}}{2C_4^2C_7 + C_5\left[2C_4C_8 + C_6\left(C_6 - \sqrt{C_6^2 + 2C_4C_8}\right)\right]} \times \ln\left[1 + z\frac{C_5\left(C_6^2 + 2C_4C_8 - C_6\sqrt{C_6^2 + 4C_4C_8}\right) + 2C_4^2C_7}{\sqrt{C_6^2 + 4C_4C_8}\left(\sqrt{C_6^2 + 4C_4C_8} - C_6\right)}\right] \quad (23)$$

The percent error associated with truncated u_b given by **equation (22)** and time calculated by **equation (23)** compared to the results obtained by **equation (20)** is less than 2.5% for depths $L \leq 5$ m, and the error decreases with the decreasing bubble volume.

Back

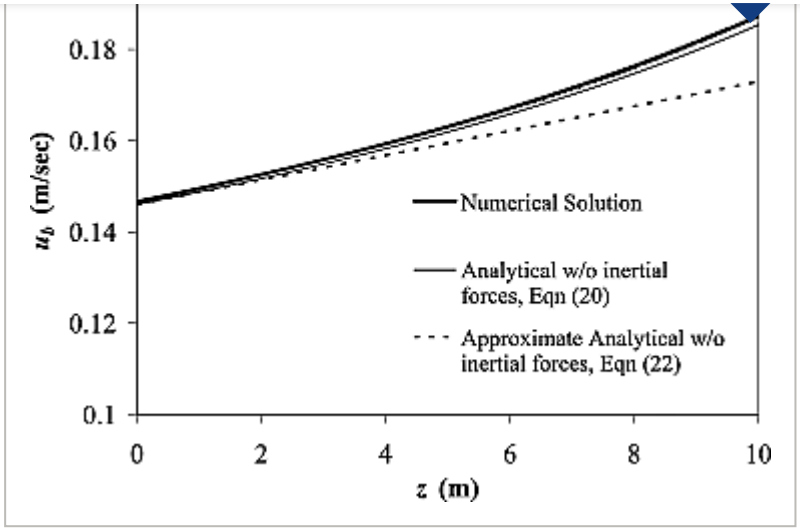

Figure 6 Open in figure viewer | PowerPoint

Comparisons of numerical and analytical solutions for R_i = 4 mm and L = 10 m.

6. Conclusions and Future Research

[24] The volume and pressure of an air bubble vary with depth as the bubble rises in a water-saturated porous medium. A balance equation of forces acting on a rising air bubble produced a second-order nonlinear ordinary differential equation, which was solved by a numerical method. Analyses of individual forces demonstrated that during the rise of compressible bubbles in a porous medium the inertial forces are negligible irrespective of the bubble volume and injection depth. The total drag force is the most dominant force to balance the buoyancy that raises the bubble. The effect of surface tension is negligible for initial equivalent bubble radii greater than 3 mm. An analytical

Back

greater depths travel with a slower rise velocity than bubbles of the equivalent volume injected at shallower depths since the higher hydrostatic water pressure results in higher drag force on the bubble. The results showed that the compressible bubble rise velocity approaches to that of the incompressible bubbles as the bubble approaches the water table. The compressible bubble velocity does not exceed 18.8 cm/s for d_p = 4 mm regardless of the injection depth and bubble volume. This conclusion is similar to the one stated by ***Corapcioglu et al.*** [2004].

[25] The analysis presented in this study indicates a definite relationship between the bubble rise velocity and the depth at which the bubble was released. Bubble velocity changes with the injection depth as a result of the compressibility of the air bubble. As the bubble rises up, it expands with decreasing pressure. Volume of a bubble injected at a 1-m depth increases 10% as the bubble reaches the water table. However, bubble volume increases almost twofold when it reaches to the surface from a depth of 10 m. In bubbly flow of air phase in coarse porous media, the theoretical results show that compressibility of air bubbles cannot be neglected except when the depth of injection is very shallow.

[26] The model developed in this study is applicable to estimate rise velocity of individual compressible bubbles whose equivalent radii range between 2 and 5 mm in water-saturated granular media. Further research is needed to compare the theoretical results presented in this study with experimental studies conducted in tall columns.

Notation

A
: Correction factor, dimensionless.

C_M
: Added mass coefficient, dimensionless.

Back

F_A
: Added mass force, N.

F_b
: Buoyant force, N.

F_d
: Total drag force, N.

F_i
: Total inertial force, N.

F_{kd}
: Kinetic drag force, N.

F_{st}
: Net surface tension force, N.

F_{vd}
: Viscous drag force, N.

g
: Gravitational acceleration, m/s^2.

L
: Elevation of the water table as measured from the injection point, m.

M
: Mass of the bubble, m^3.

n
: Number of moles of air, mol.

P
: Pressure in the bubble, N/m^2.

P_0
: Atmospheric pressure, N/m^2.

R
: Universal gas constant, J/mol/K°.

Back

R_g
: The gas constant for air, J kg/K°.

R_i
: Equivalent bubble radius at the injection point, m.

R'
: Pore throat radius, m.

T
: Temperature, K°.

t
: Time, s.

t_L
: Travel time to reach the water table, s.

u_b
: Bubble rise velocity, m/s.

z
: Vertical distance to the center of the bubble, m.

$\forall_b$
: Volume of a bubble, m^3.

$\forall_{ib}$
: Initial bubble volume at the injection point, m^3.

ρ_g
: Density of air, kg/m^3.

ρ_f
: Density of water, kg/m^3.

σ
: Surface tension, N/m.

β
: Compressibility of air, 1/Pa.

Back

θ_R
: Receding contact angle, radian.

θ_A
: Advancing contact angle, radian.

μ_b
: Dynamic viscosity of an air bubble, N.s/m^2.

μ_f
: Dynamic viscosity of water, N.s/m^2.

ϕ
: Porosity, %.

Acknowledgments

[27] This research was sponsored by a grant from TUBITAK. The authors wish to thank to John Tyner for his comments during the preparation of the manuscript.

Supporting Information

Filename	Description
wrcr11050-sup-0001-t01.txt plain text document, 296 B	Tab-delimited Table 1.

Please note: The publisher is not responsible for the content or functionality of any supporting information supplied by the authors. Any queries (other than missing content) should be directed to the corresponding author for the article.

Back

Amos, R. T., and K. U. Mayer (2006), Investigating ebullition in a sand column using dissolved gas analysis and reactive transport modeling, *Environ. Sci. Technol.*, **40**, 5361–5367.

CAS | ADS | PubMed | Web of Science® | Google Scholar

Bankoff, S. G. (1972), Growth of a vapor bubble in a porous medium, in *Fundamentals of Transport Phenomena in Porous Media*, pp. 161–296, Elsevier, New York.

Google Scholar

Batchelor, G. K. (2000), *An Introduction to Fluid Dynamics*, 615 pp., Cambridge Univ. Press, New York.

Google Scholar

Bird, R. B., W. E. Stewart, and E. N. Lightfoot (2002), *Transport Phenomena*, 2nd ed., John Wiley, New York.

Google Scholar

Brooks, M. C., W. R. Wise, and M. D. Annable (1999), Fundamental changes in in-situ air sparging flow patterns, *Ground Water Monit. Rem.*, **19**, 105–113.

Web of Science® | Google Scholar

Back

ADS | Web of Science® | Google Scholar

Ergun, S. (1952), Fluid flow through packed columns, *Chem. Eng. Prog.*, **48**, 89–94.

CAS | Web of Science® | Google Scholar

Garrettson, B. A. (1973), Bubble transport theory with application to the upper ocean, *J. Fluid Mech.*, **59**, 187–206.

ADS | Web of Science® | Google Scholar

Hilsenrath, J., et al. (1955), Tables of thermal properties of gases, *Natl. Bur. Stand. Circ. 564*, U. S. Gov. Print. Off., Washington, D. C.

Google Scholar

Landau, L. D., and E. M. Lifshitz (1987), *Fluid Mechanics*, 2nd ed., 539 pp., Elsevier, Oxford, U. K.

Google Scholar

LeBlond, P. H. (1969), Gas diffusion from ascending gas bubbles, *J. Fluid Mech.*, **35**, 711–719.

ADS | Web of Science® | Google Scholar

Back

Google Scholar

Li, X., and Y. C. Yortsos (1995), Visualization and simulation of bubble growth in pore networks, *AIChE J.*, **41**, 214–222.

CAS | Web of Science® | Google Scholar

Oldenburg, C. M., and J. L. Lewicki (2006), On leakage and seepage of CO_2 from geologic storage sites into surface water, *Environ. Geol.*, **50**, 691–705.

CAS | ADS | Web of Science® | Google Scholar

Pankow, J. F., R. L. Johnson, and J. A. Cherry (1993), Air sparging in gate wells in cutoff walls and trenches for control of plumes of volatile organic compounds (VOCs), *Ground Water*, **31**, 654–663.

CAS | Web of Science® | Google Scholar

Wallis, G. B. (1969), *One-Dimensional Two-Phase Flow*, 219 pp., McGraw-Hill, New York.

PubMed | Google Scholar

Winterton, R. H. S. (1984), Flow boiling: Prediction of bubble departure, *Int. J. Heat Transfer*, **27**, 1422–1424.

CAS | Web of Science® | Google Scholar

Back

Citing Literature

Download PDF

Back to Top

Back

and Publishing Policies